32nd Electric Vehicle Symposium (EVS32)
Lyon, France, May 19 - 22, 2019

Influence of Different Charging Rates on Li-ion Battery Lifespan: Experimental Validation

Jorge Nájera[1], Jaime R. Arribas[1], Marcos Lafoz[2], Pablo Moreno-Torres[1], Rosa M. de Castro[1]

[1]*Escuela Técnica Superior de Ingenieros Industriales, Universidad Politécnica de Madrid, 28006 Madrid, Spain; jorge.najera.alvarez@alumnos.upm.es*

[2]*CIEMAT, Government of Spain, 28040 Madrid, Spain*

Summary

The impact of different charging rates on an EV battery has been investigated in this article. Taking into consideration the battery temperature and the charging profile, it has been shown that the charging rate has a considerable influence on battery lifespan. This issue, already known in the fast charging environment due to the chemical limitations of the battery, has been satisfactory reproduced by the battery ageing model in the paper. Simulation studies have been carried out based on a battery aging model which has been validated with laboratory tests. Results indicate that fast charging requires an appropriate cooling system in order to ensure the temperature control for avoiding the premature ageing of the battery.

Keywords: battery ageing, lithium battery, charging.

1 Introduction

It is well known that transportation has a huge effect on greenhouse gases linked to global climate change. According to the US Environmental Protection Agency (EPA), transportation sector generates the largest share of greenhouse gas emissions, nearly 28.5% [1]. Besides, passenger cars and light-duty trucks account for over half of the emissions from the transportation sector. Due to this situation, reducing transportation emissions has become one of the key issues for Governments. For instance, Horizon2020 European research program accounts for several goals related with diminish passenger cars emissions, and various types of clean energy transportation systems such as Battery Electric Vehicles (BEV) or Plugin Hybrid Electric Vehicles (PHEVs) have been developed [2].

In recent years, high energy lithium ion batteries integrated in a battery pack have caught attention for the applications on electrical vehicles (EVs) and hybrid electrical vehicles which demand a high-energy and high-power energy storage system [3]. However, energy storage systems (ESSs) are still the critical issue for electric transportation since it suffers from various stress factors such as high charging and discharging current rates or extreme operating temperatures [4]. Battery ageing while discharging depends highly on the driver profile, so ageing while charging becomes critical since it is a standardized process where EV owner does not intervene. Due to battery importance and high cost, there is a need for a comprehensive study of the ageing phenomena in the battery when charging with different rates, so the aging during that common process is minimized and the battery lifespan can be extended as much as possible.

Lithium-ion batteries aging process has already been studied, and different models have been developed accounting for various aging processes: parasitic side reactions, electrolyte interface formation, and resistance increase [5-7]. Versatile models that consider several of these effects are as well published in [8-9].

This paper aims to validate a modified ageing model through experimental simulation and study the influence of different charging rates on a Li-ion battery lifespan.

2 Methodology

The mathematical battery model used for simulation analysis is described next, as well as the laboratory facilities and the test procedure to validate the aging model.

2.1 Battery model

2.1.1 Voltage-Current Performance and Runtime Model

The lithium-ion battery model used in this paper is a modification of the Mathworks model in the SimPower toolbox from MATLAB Simulink, which has been previously published in [8] and [9]. The equivalent circuit is based on the Shepherd model [10], which was developed and validated in [11] and [12]. Although more accurate and complete equivalent circuits have been proposed [13], this model keeps error between 1 and 5% and does not require to test the battery to obtain parameters, since it is sufficient with the datasheet information. In this paper, the battery model is based on the one described in [12], including thermal dependencies and modelling the internal resistance as two different resistances, ohmic and polarization resistance, the latter being dependent on the State of Charge (SoC) (Figure 1).

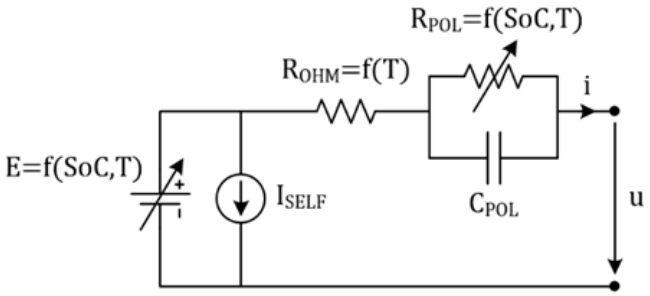

Figure 1: Battery equivalent circuit [1]

The model behaves as follows:

$$E = f(SoC) = E_0 - K \cdot Q_{MAX}\left(\frac{100}{SoC} - 1\right) + A \cdot e^{-B \cdot Q_{MAX}\left(1-\frac{SoC}{100}\right)} \quad (1)$$

$$R_{POL,discharge} = f(SoC) = K\frac{100}{SoC} \quad (2)$$

$$R_{POL,charge} = f(SoC) = K\frac{1}{1.1 - \frac{SoC}{100}} \quad (3)$$

where u is the battery instantaneous voltage [V], i is the battery current [A] ($i > 0$ discharging; $i < 0$ charging), SoC is battery state of charge [%], I_{SELF} is the self-discharge current [A], R_{OHM} is the ohmic internal resistance [Ω], R_{POL} is the polarization internal resistance [Ω], C_{POL} is the polarization capacitor [F], E is the open-circuit nonlinear voltage [V], E_0 is the open-circuit constant voltage [V], K is the polarization constant [Ω], Q_{MAX} is the maximum capacity [Ah], A is the exponential voltage constant [V], and B is the exponential capacity constant [Ah-1].

2.1.2 Thermal Model

The thermal model implemented comprises two parts: a heat generation model, and a heat evacuation model, the former published in [14]:

$$H = (E_0 - E)i + T\frac{dE}{dT}i + (R_{OHM} + R_{POL})i^2 \tag{4}$$

where H is the heat generated [W], T [K] is the temperature and $dE/dT \gtrless 0$ is the change of the equilibrium potential with temperature, which is dependent on the SoC [15]. As aforementioned, parameters from equations (1), (2) and (3) are temperature dependent:

$$E_0(T) = E_0(T_0) + \frac{dE}{dT}(T - T_0) \tag{5}$$

$$Q_{MAX}(T) = Q_{MAX}(T_0) + \frac{dQ}{dT}(T - T_0) \tag{6}$$

$$K(T) = K(T_0) \cdot e^{\alpha\left(\frac{1}{T} - \frac{1}{T_0}\right)} \tag{7}$$

$$R_{OHM}(T) = R_{OHM}(T_0) \cdot e^{\beta\left(\frac{1}{T} - \frac{1}{T_0}\right)} \tag{8}$$

The heat evacuation model, which was published in [16], assumes that the only heat transfer to be modelled is that from the cell surface to the ambient. Therefore, the temperature variation for a single cell can be obtained as follows:

$$H \approx m \cdot c_p \frac{dT}{dt} + \frac{1}{R_{OUT}}(T - T_0) + E \cdot \sigma \cdot (T^4 - T_0^4) \Rightarrow R_{OUT} = \frac{1}{h \cdot Ar} \tag{9}$$

$$T(s) = \frac{H \cdot R_{OUT} + T_0}{1 + m \cdot c_p \cdot R_{OUT} \cdot s} = \frac{H \cdot R_{OUT} + T_0}{1 + t_{th} \cdot s} \tag{10}$$

where m and c_p $[J \cdot kg^{-1} \cdot K^{-1}]$ are the mass and the specific heat capacity of the cell, h $[W \cdot m^{-2} \cdot K^{-1}]$ is the convective heat transfer coefficient, Ar is the external surface area of one cell, T_0 is the ambient temperature, σ is the Stefan-Boltzmann constant, and t_{th} [s] is the thermal time constant.

2.1.3 Aging Model

Battery aging has also been included in the model developed during this work for cycle life estimation purposes, neglecting calendar aging [17]. Lithium-ion batteries aging models are strongly dependent on the cathode chemistry, i.e., they are not valid for every type of lithium-ion battery but for a specific one. As explained in the next subsection, the lithium-ion batteries tested in this paper are of $LiNi_xCo_yMn_zO_2$ chemistry. An aging model for this chemistry was developed in [18], based on experimental results. The capacity loss can be calculated as follows:

$$Q_{loss} = (aT^2 + bT + c) \cdot e^{(d \cdot T + e)C_{rate}} \cdot Ah \tag{11}$$

where Q_{loss} is the lost capacity [Ah], C_{rate} is the charge/discharge current with respect to the nominal capacity, and Ah is the capacity that has been extracted and/or injected into the battery.

The rest of the parameters are calculated based on experimental results and can be obtained from [18]. Besides, the temperature can be calculated as stated in equation (10).

The model has been validated in [18] for constant discharge current and for a single cell. Laboratory tests described in the next subsection aim to validate the aging model for different charging rates, and for a battery pack which is composed by 14 cells.

2.2 Laboratory test

The power system of the test bench used for the laboratory tests is shown in Figure 2 [19-20]. It consists of the $LiNi_xCo_yMn_zO_2$ battery, a DC/DC power electronic converter, a DC/AC power electronic converter, and a transformer connected to the 400 V grid. This topology allows to exchange power between the grid and the batteries.

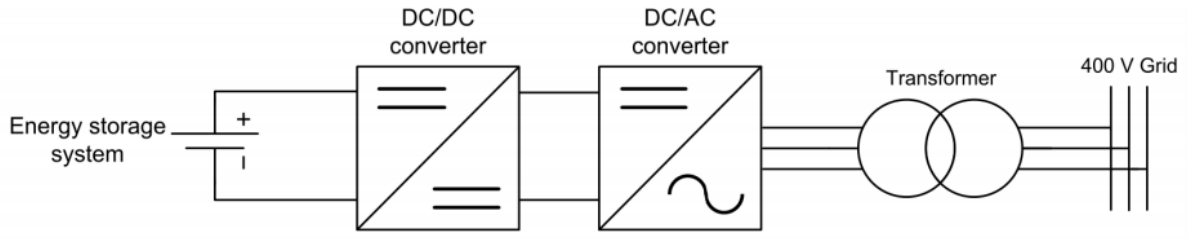

Figure 2: Test bench scheme [11]

The control hardware comprises both electrical and thermal measurements, a digital signal processor (DSP) and a computer that acts as a Human-Machine interface. The DC/DC converter is responsible for controlling the current in the battery through a PWM current control strategy with a constant switching frequency of 5 kHz. The DC/AC converter is controlled as a conventional grid-tie inverter with reactive power control capability. This converter is responsible for controlling both the DC voltage in the DC link and the reactive power exchanged with the grid (direct-sequence control), although this reactive power capability is not relevant for the aging studies presented in this paper. The DC/AC converter control strategy is a SVPWM current control with a constant switching frequency of 5 kHz. In order to guarantee a proper behaviour of the test bench, the rated voltage of the batteries must be comprised between 12 and 96 V. The rated power of the two electronic converters is 15 kV, and the batteries are located inside a safety room.

The battery pack used both for simulations and test consist of 14 Li-polymer cells connected in series, where each cell has a rated capacity of 55 Ah and a nominal voltage of 3.7 V [21]. Hence, the battery pack nominal voltage equals 51.8 V. Scenarios shown in Table 1 have been defined to validate the model for different charging rates, both for simulation and experimental test. Cycling should be performed from 80% to 20% SoC for each charging mode while keeping the discharge current rate constant, so results related to different charging modes can be extracted. Ambient temperature is kept between 23±3ºC. Since battery cycling and capacity fade tests are time demanding, only 100 slow charging cycles have been performed by the time this paper is published. In order to fully validate the aging model, semi-fast and fast cycling tests need to be performed once the slow cycling is finished. Moreover, different temperatures should be taken into consideration as well. At last, non-constant charging/discharging patterns will be tested.

Table1: Charging rate scenarios

	Discharge (C)	Charge (C)	SoC range	Ambient temperature
Slow	1	0.5		
Semi-fast	1	1.5	20% - 80%	23±3ºC
Fast	1	3		

3 Aging model experimental validation

Figure 3 shows capacity fade evolution after 100 cycles with slow charge (1C discharge and 0.5C charge), from 20% to 80% SoC. Capacity tests were performed at 50 and 100 cycles, three times at each number of cycles for sake of repeatability. As stated by the battery manufacturer in [21], a capacity test is completed when the battery is discharged at C/3 from the fully charged open circuit voltage to cut-off voltage. Aging model simulations were carried out in the environment of MATLAB Simulink SimPowerSystems.

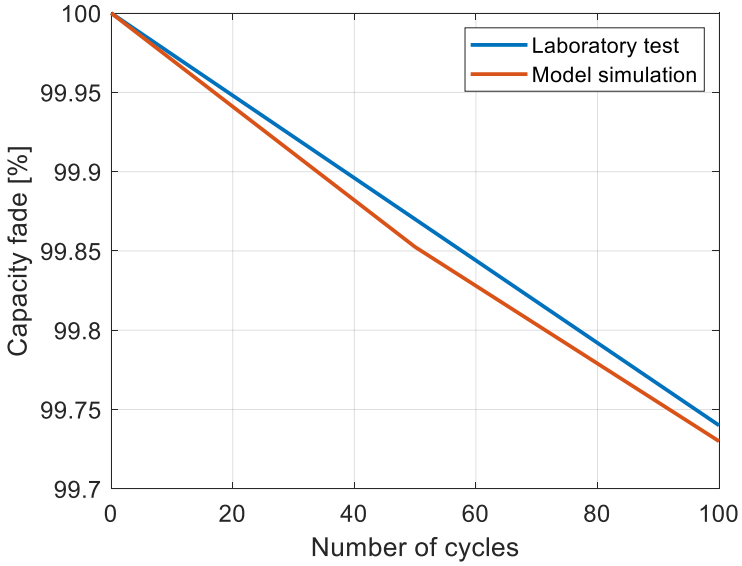

Figure 3: Capacity fade after 100 cycles between 20% and 80 % SoC, charging at 0.5C and discharging at 1C.

The model predicts a capacity fade of 0.26%, while the tendency line of the laboratory test reaches 0.27 % after 100 cycles. The relative error is less than 5%. As aforementioned, laboratory test with different charging rates, at different temperatures and with different discharging profiles need to be performed in order to fully validate the aging model. Nevertheless, [22] and [23] suggest that the validation performed in [18] can be extended to a battery pack and for different charging rates.

4 Influence of charging rate in battery lifespan

Once the ageing model of the battery has been validated accurately enough with the experimental set of batteries, the next analysis will be accomplished using the model.

In order to study the influence of different charging rates on the battery lifespan, simulation studies have been carried out comparing slow, semi-fast and fast charging rates. The discharge current is kept constant and equal to 1C for every simulation, so its aging effect should be the same in all cases. Simulation scenarios have been defined based on two variables: temperature and charging profile.

Regarding temperature, the absence or presence of a cooling system in the battery is taken into consideration. On the one hand, if the battery accounts for a high-performance cooling system the battery temperature is assumed to be constant and equal to ambient temperature (23ºC). On the other hand, if there is no cooling system or the cooling system is not able to assume the temperature increase of high current charge, the battery temperature will vary based on the thermal model previously described. Regarding the charging profile, constant current/constant voltage (CC/CV) and constant current (CC) charging profiles have been considered. When charging with CC/CV type, charging is performed at the corresponding current (C-rate from Table 1) until SoC reaches 80%, and then the current decreases while keeping the voltage constant until the battery is fully charged. CC charging profile keeps charging the battery at the same rate until SoC equals 100%%, producing negative thermal effects in the battery when charging with high current levels. Based on the absence or presence of a cooling system and the charging profile, the following four scenarios have been defined:

Table2: Simulation scenarios

	Cooling system	Charging profile
Scenario I	No	CC/CV
Scenario II	Yes	CC/CV
Scenario III	No	CC
Scenario IV	Yes	CC

Figure 4 shows battery aging, presented as capacity fade in % after 1000 cycles, for the four selected scenarios, considering in each case the three charging rates (slow, semi-fast and fast).

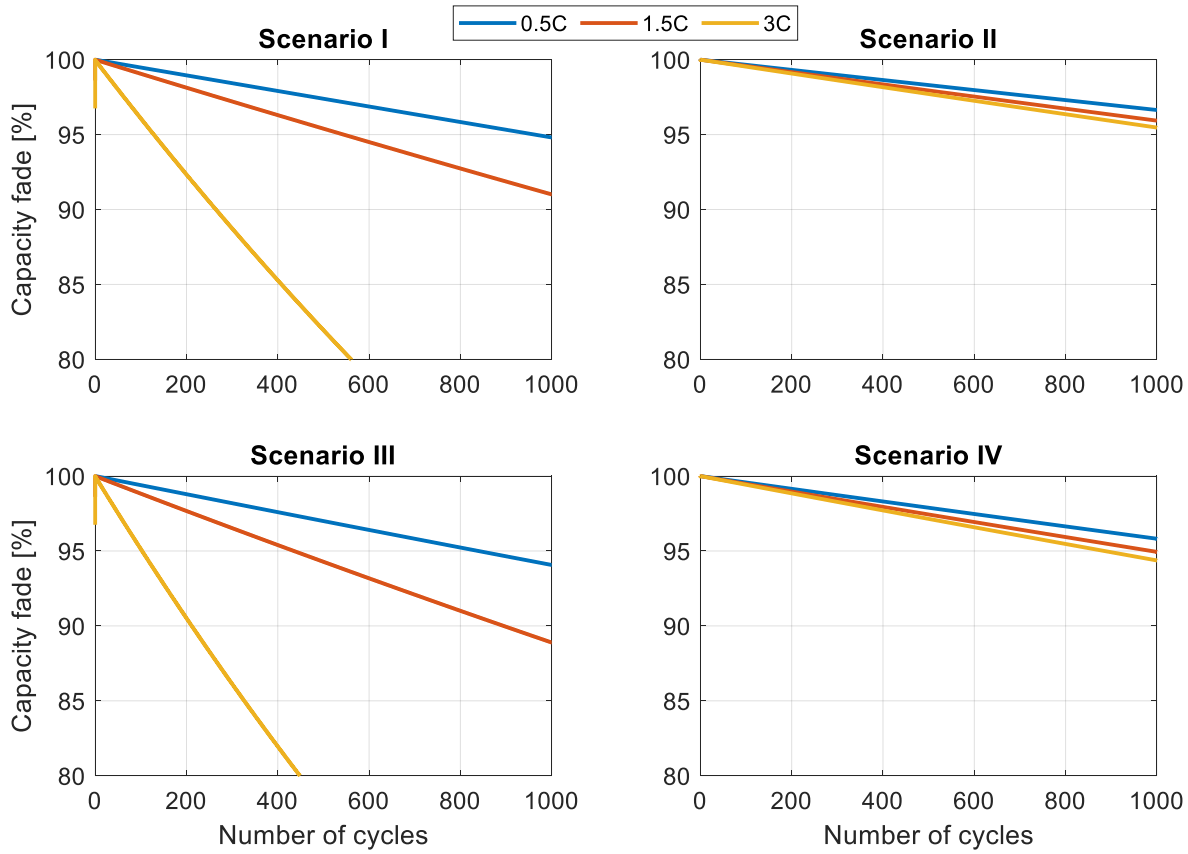

Figure 4: Simulation results for the selected scenarios and for the three charging rates (0.5C – 1.5C – 3C).

As expected, the cycling aging is most severe with fast charging in all scenarios. Regarding temperature dependency, scenarios with no cooling system are represented in Figures 4(a) and 4(c), while scenarios equipped with refrigeration are displayed in Figures 4(b) and 4(d). It can be derived from these figures that fast charging is highly inconvenient for the battery lifespan when it does not account for an appropriate cooling system. For both scenarios I and III, the battery capacity reaches the end of life value of 80% at 561 and 449 cycles respectively, while for scenarios II and IV the capacity fade is only 1.5% higher than the one achieved by the slow charge. Semi-fast charge can also be considered detrimental without refrigeration, since battery lifespan prognosis is close to 2000 cycles for both CCCV and CC charging profiles (Figures 4(a) and 4(c)). On the other hand, capacity fade with slow charging and no cooling system is not critical, although improvements in capacity of 2% per 1000 cycles can be observed if the battery is refrigerated.

Charging profile influence on battery lifespan is less significant than temperature. Capacity fade differences of less than 2% per 1000 cycles can be observed between scenarios with CCCV and CC charging profile, for the cycling pattern defined in this work.

At last, fast charging simulations for the different scenarios are summarized in Figure 5. As expected, scenario II (cooling system and CCCV charging profile) reduces the capacity fade with respect to the rest of scenarios. It is clear that, when dealing with fast charges, refrigerating the battery becomes vital and necessary in order to extend as much as possible the battery life.

Simulation results are summarized in Table 3. The charging method that most preserves the battery life consist of slow charge with a cooling system and CCCV charging profile. Nevertheless, semi-fast and fast charge for scenario II provide similar results, and they could be a better solution if user comfort and charging time are taken into consideration.

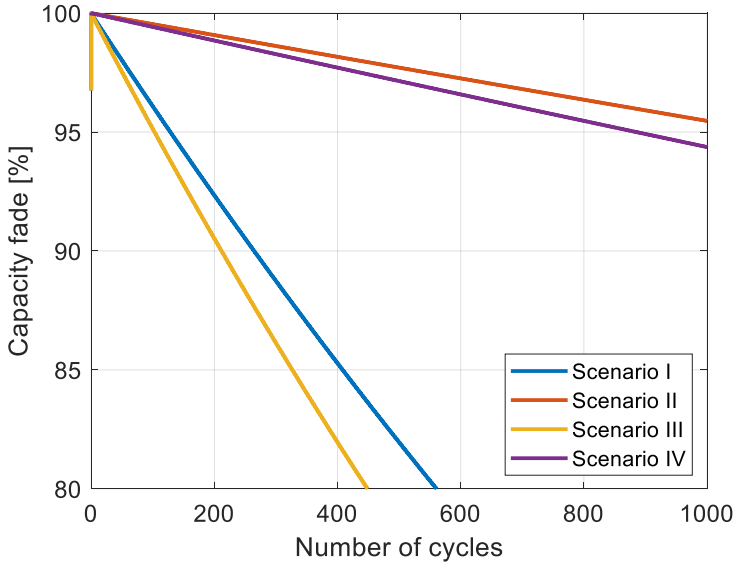

Figure 4: Simulation results when charging with 3C.

Table3: Simulation results after 1000 cycles

	Charging rate	Capacity fade after 1000 cycles
Scenario I *No cooling* *CCCV*	Slow	94,8%
	Semi-fast	91,0%
	Fast	80% at 561 cycles
Scenario II *Cooling* *CCCV*	Slow	96,6%
	Semi-fast	95,9%
	Fast	95,4%
Scenario III *No cooling* *CC*	Slow	94,0%
	Semi-fast	88,8%
	Fast	80% at 449 cycles
Scenario IV *Cooling* *CC*	Slow	95,8%
	Semi-fast	94,9%
	Fast	94,3%

5 Conclusions

In this article, the impact of different charging rates on an EV battery has been investigated. Taking into consideration the battery temperature and the charging profile (CCCV or CC), it has been shown that, as expected, the charging rate has a considerable influence on battery lifespan. Simulation studies have been carried out based on a battery aging model which has been validated with laboratory tests. The battery pack used both for simulations and test consist of 14 Li-polymer cells connected in series, where each cell has a rated capacity of 55 Ah and a nominal voltage of 3.7 V.

Results indicate that fast charging requires an appropriate cooling system in order to ensure the temperature control for avoiding the premature ageing of the battery. Moreover, it is highly recommended not to carry out the charge at constant current over the 80% of SoC. This issue, already known in the fast charging environment due to the chemical limitations of the battery, has been satisfactory reproduced by the battery ageing model in the paper. Among the two effects the temperature one becomes more relevant, since capacity fade when the cooling system is not suitable is extremely severe, reaching the end of life value (80%) in less than 600 cycles for fast charging. This effect can be observed with semi-fast charging as well, with a capacity fade difference of 6% when comparing scenarios that account for an appropriate cooling system with scenarios that lack of it. On the other hand, the importance of the charging profile is not severe, specially

when the cooling system is well designed. Capacity fade differences of 2% per 1000 cycles for fast-charging, 1% for semi-fast charging, and 0.8% for slow charging when comparing CC charging profile scenarios with CCCV charging profile. As a conclusion, semi-fast and fast charging can be considered as non-critical charging strategies if the battery is properly cooled.

Acknowledgments

This work was partially supported by the following project: 'SEGVAUTO 4.0 - CM. Convocatoria de Programas de I+D en Tecnología/2018 Orden 4411/2018, de 13 de diciembre, Reference: S2018/EMT-4362'.

References

[1] *EPA*, https://www.epa.gov/ghgemissions, accessed on 2018-10-29.

[2] *Horizon2020*, http://ec.europa.eu/programmes/horizon2020/, accessed on 2018-10-29..

[3] Ye, Yonghuang, et al. "Effect of thermal contact resistances on fast charging of large format lithium ion batteries." *Electrochimica Acta* 134 (2014): 327-337.

[4] Omar, Noshin, et al. "Lithium iron phosphate based battery–assessment of the aging parameters and development of cycle life model." *Applied Energy* 113 (2014): 1575-1585.

[5] Ramadass, P., et al. "Development of first principles capacity fade model for Li-ion cells." *Journal of the Electrochemical Society* 151.2 (2004): A196-A203.

[6] Spotnitz, Robert. "Simulation of capacity fade in lithium-ion batteries." *Journal of Power Sources*113.1 (2003): 72-80.

[7] Dubarry, Matthieu, et al. "Capacity loss in rechargeable lithium cells during cycle life testing: The importance of determining state-of-charge." *Journal of Power Sources* 174.2 (2007): 1121-1125.

[8] Nájera, Jorge, et al. "Approach to hybrid energy storage systems dimensioning for urban electric buses regarding efficiency and battery aging." *Energies* 10.11 (2017): 1708.

[9] Moreno-Torres Concha, Pablo. *Analysis and Design Considerations of an Electric Vehicle Powertrain regarding Energy Efficiency and Magnetic Field Exposure*. Doctoral Dissertation. Universidad Politécnica de Madrid, 2016.

[10] Shepherd, Clarence M. "Design of primary and secondary cells II. An equation describing battery discharge." *Journal of the Electrochemical Society*112.7 (1965): 657-664.

[11] Tremblay, Olivier, Louis-A. Dessaint, and Abdel-Illah Dekkiche. "A generic battery model for the dynamic simulation of hybrid electric vehicles." *2007 IEEE Vehicle Power and Propulsion Conference*. Ieee, 2007.

[12] Tremblay, Olivier, and Louis-A. Dessaint. "Experimental validation of a battery dynamic model for EV applications." *World electric vehicle journal* 3.2 (2009): 289-298.

[13] Chen, Min, and Gabriel A. Rincon-Mora. "Accurate electrical battery model capable of predicting runtime and IV performance." *IEEE transactions on energy conversion* 21.2 (2006): 504-511.

[14] Saw, L. H., et al. "Electro-thermal analysis of Lithium Iron Phosphate battery for electric vehicles." *Journal of Power Sources* 249 (2014): 231-238.

[15] Forgez, Christophe, et al. "Thermal modeling of a cylindrical LiFePO4/graphite lithium-ion battery." *Journal of Power Sources* 195.9 (2010): 2961-2968.

[16] Chen, Yufei, and James W. Evans. "Three-Dimensional Thermal Modeling of Lithium-Polymer Batteries under Galvanostatic Discharge and Dynamic Power Profile." *Journal of the Electrochemical Society* 141.11 (1994): 2947-2955.

[17] Barré, Anthony, et al. "A review on lithium-ion battery ageing mechanisms and estimations for automotive applications." *Journal of Power Sources* 241 (2013): 680-689.

[18] Wang, John, et al. "Degradation of lithium ion batteries employing graphite negatives and nickel–cobalt–manganese oxide+ spinel manganese oxide positives: Part 1, aging mechanisms and life estimation." *Journal of Power Sources* 269 (2014): 937-948.

[19] Concha, P., et al. "Energy storage systems for electric vehicles: Performance comparison based on a simple equivalent circuit and experimental tests." *World Electric Vehicle Journal* 6.3 (2013): 592-602.

[20] Concha, P., et al. "Flexible low-cost system to test batteries and ultracapacitors for electric and hybrid vehicles in real working conditions." *2013 World Electric Vehicle Symposium and Exhibition (EVS27)*. IEEE, 2013.

[21] Kokam*, Technical Specification: SLPB100255255HR2.*

[22] Shen, Junyi, Serkan Dusmez, and Alireza Khaligh. "Optimization of sizing and battery cycle life in battery/ultracapacitor hybrid energy storage systems for electric vehicle applications." *IEEE Transactions on industrial informatics* 10.4 (2014): 2112-2121.

[23] Zhu, Cong, et al. "Development of a theoretically based thermal model for lithium ion battery pack." *Journal of Power Sources* 223 (2013): 155-164.

Authors

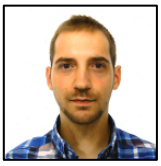

Jorge Nájera received the MSc degree in electrical engineering from Universidad Politécnica de Madrid, Madrid, Spain in 2015. He is doing his Ph.D. studies at Universidad Politécnica de Madrid, within the Department of Electrical Engineering. His research interests include Li-ion battery modelling, hybrid energy storage systems, and integration of non-conventional power sources into the power grid.

Jaime Rodríguez Arribas received the Ph.D. degree in electrical engineering from the Universidad Politécnica de Madrid, Madrid, Spain, in 2000. Since 1992, he has been with the Department of Electrical Engineering, Universidad Politécnica de Madrid, teaching graduate and postgraduate courses in electrical machines and their control. His mayor field in research activities deal with renewable energy generation and the power train of EVs.

Marcos Lafoz received the Ph.D. M.S. degree in electrical engineering from the Universidad Politécnica de Madrid (Spain) in 2005. He works as scientific researcher in the Spanish public research center CIEMAT from 2008. His research interests include electric power drives design and control, power electronic converters, wave energy generation, and energy storage used both for electric vehicles and renewable energy integration.

Pablo Moreno-Torres received the Ph.D. degree in electrical engineering from the Universidad Politécnica de Madrid in 2016. He works as a power electronics engineer at Siemens Gamesa from 2018, and as assistant professor at the Universidad Politécnica de Madrid from 2017. His fields of expertise are power electronics, batteries, supercapacitors, electrical machines and electrical drives. He has worked in projects belonging to the fields of electric vehicles, renewable energies and energy storage systems. He also has experience teaching university courses and technical courses.

Rosa M. de Castro received the Ph.D. degree in electrical engineering from the Universidad Politécnica de Madrid (Spain) in 2013. She joined the Department of Electrical Engineering at Universidada Politécnica de Madrid in 2001, where she is currently an Associate Professor. Her research interests include power system analysis, voltage stability and integration of renewable energy sources into distribution grids.